PERGAMON

Aerosol Science 32 (2001) 975–991

Journal of
Aerosol Science

www.elsevier.com/locate/jaerosci

Counting efficiency of condensation particle counters at low-pressures with illustrative data from the upper troposphere

M. Hermann*, A. Wiedensohler

Institute for Tropospheric Research, Permoserstr. 15, 04303 Leipzig, Germany

Received 16 June 2000; accepted 9 January 2001

Abstract

The low-pressure counting efficiency of three modified condensation particle counters (CPCs, TSI Model 7610) was investigated. In this study, we describe the modifications of the counters, present a "new" low-pressure calibration set-up, and show the resulting CPC counting efficiency curves as function of operating pressure (160–1000 hPa) and temperature difference between the saturator and condenser block (10.5–26.0°C). Furthermore, particle coincidence in the CPC optics was studied. The presented CPCs are able to measure particle number concentrations of up to 40,000 particles/cm^3 at pressures down to 160 hPa. The lower threshold diameter of the CPCs can be varied between 4 and 23 nm. © 2001 Elsevier Science Ltd. All rights reserved.

1. Introduction

Particle number concentrations in the submicrometer size range smaller than 20 nm can be obtained using a combination of condensation particle counters (CPCs) with different lower detection limits. In such a combination, each counter measures the integral particle number concentration of all particles larger than a certain threshold diameter. By using CPCs with different threshold diameters, information on the particle size distribution is obtained in the size range accessible by the CPC thresholds.

Since the CPCs in a CPC combination measure simultaneously, the time resolution of such a system is in the order of seconds which is at least one order of magnitude higher than for

* Corresponding author. Tel.: + 49-341-235-2918; fax: + 49-341-235-2361.
E-mail address: hermann@tropos.de (M. Hermann).

0021-8502/01/$ - see front matter © 2001 Elsevier Science Ltd. All rights reserved.
PII: S0021-8502(01)00037-4

comparable systems. The high time resolution is an important advantage in measuring aerosols with a high temporal variability. The major disadvantage of a combination of several CPCs is, however, the limited size resolution.

One important application of such a CPC combination lies in aircraft-borne measurements. CPCs are, on account of their high time resolution, well suited for measurements at high aircraft speed. The low operating pressures down to 150–200 hPa, however, may cause problems in the performance of the counters. Although single CPCs or combinations of CPCs have been used for aircraft-borne measurements by several scientific groups (e.g. Clarke, 1993; Schröder & Ström, 1997; Cofer, Anderson, Winstead, & Bagwell, 1998; Brock et al., 2000) only very few low-pressure calibrations of these instruments have been performed. This is mainly due to problems entailed with the generation of a well-defined aerosol at lower pressure and the precise measurement of that aerosol. Consequently, most of these CPC systems were poorly characterized and no or only sparse data on their performance at flight pressures have been published.

For the CPC 3020, Heintzenberg and Ogren (1985), Dreiling and Jaenicke (1988), and Saros, Weber, Marti, and McMurry (1996) carried out calibration experiments. Zhang and Liu (1990) performed theoretical calculations on the counting efficiency of this CPC. The TSI models 3025 and 3760 were calibrated by Cofer et al. (1998), but only at one pressure (213 hPa). Another calibration of the CPC 3760 was performed by Noone and Hansson (1990). They determined the integral counting efficiency in the pressure range of 160–1000 hPa. The only study where the CPC counting efficiency was investigated both size resolved and in dependence on operating pressure is reported by Zhang and Liu (1991).

In the present study, we describe the modifications of three TSI CPCs 7610 (TSI Inc., St. Paul, MN, USA) and the experimental set-up used to measure the low-pressure counting efficiency of the instruments. We present counting efficiency curves as function of operating pressure (160–1000 hPa) and temperature difference between the saturator and condenser block (10.5–26.0°C) and compare these curves with data from the literature. In further experiments, particle coincidence in the CPC optics was studied in order to expand the upper concentration range limit of the particle counters. As an illustration, obtainable with a CPC combination, we finally present one example of data of measurements taken aboard an aircraft in the upper troposphere.

2. Experimental

CPCs are designed to count particles which are normally too small to be directly detected by light scattering (diameter $<$ ca. 100 nm). To measure these small particles, in the present CPC type, a continuous aerosol flow is saturated with butanol vapor in the saturator block of the CPC. Downstream the saturator, the aerosol flow is cooled in the condenser block which results in high supersaturation with respect to the butanol vapor. Consequently, the particles grow by butanol condensation to particle diameters of several micrometers. The enlarged particles are finally counted by a laser-photodiode optics next to the condenser.

The performance of a CPC can be characterized by its counting efficiency curve which is a function of particle size and CPC operating parameters (cf. Fig. 2). The counting efficiency η is defined as the ratio of the particle number concentration counted by the CPC to the given particle

number concentration. The shape of the counting efficiency curve is determined by the supersaturation profile within the condenser. This profile depends mainly on three CPC operating parameters: the operating pressure, the temperature difference between the saturator and condenser block, and the volume flow rate through the instrument. To characterize the counting efficiency curve, usually the lower particle size detection limit or threshold diameter d_{50} and the asymptotic maximum counting efficiency $\eta_{\max}$ for particles much larger than the threshold diameter is used. The threshold diameter d_{50} can be defined as the particle diameter, where 50% of the asymptotic maximum counting efficiency is reached. Due to boundary layer effects and diffusive and phoretic particle losses, the asymptotic maximum counting efficiency is slightly below 100%.

2.1. CPC modifications

Since commercially available CPCs are not designed for low-pressure applications, the counters used in this study had to be modified. Furthermore, the originally equal threshold diameters of the three instruments had to be shifted to gain a certain sizing capability.

In a first step, each CPC was made vacuum tight to guarantee a proper functioning at lower pressures encountered at flight altitude. In particular, the 3/8 in. CPC inlet tube and the quick fit connectors at the rear, used for filling the counters with butanol, were found to be major leaks. The purge air flow, normally necessary for clean room applications, was sealed off to keep the pressure downstream the orifice low enough for critical operation. To monitor the saturator and condenser temperatures, additional temperature sensors were installed. For stability against vibrations during airborne use, all connectors and larger electronic components (e.g. the photodetector and laser board) were secured with silicon adhesive.

The saturator of a TSI CPC 7610 consists of a hollow aluminum block which is used as butanol bath. A part of this cavity is occupied by an open pore plastic sponge which has a flow tube for the aerosol at its center line. When the bath is filled with butanol, the alcohol is sucked into the sponge and the aerosol flow is saturated with butanol vapor. For aircraft application, two additional sponges were added to prevent the butanol to swash around during flight. This measure minimizes the risk of contamination of the CPC optics by butanol.

The original CPCs 7610 have a tube connection between the flow tube inside the sponge and the bath which guarantees equal pressure in both reservoirs. If the tube is blocked or missing, a pressure decrease at the CPC inlet forces butanol out of the sponge into the flow tube. Hence, butanol is sucked through the optics which causes a malfunctioning of the CPC.

Originally, the pressure equalizing tube in the CPC 7610 has a filter inside to prevent particles from the bath to enter the flow tube and be counted afterwards. This filter proved to be a major problem for aircraft applications. On account of the strong pressure changes during aircraft ascent and descent, the filter becomes clogged with butanol which prevents further pressure equalization.

To overcome this problem, a new pressure equalizing tube without a filter was installed. This 1/8″ stainless steel tube connects the CPC inlet directly with the butanol bath, but has also a branch which leads via a critical orifice to a vacuum pump. The volume flow through this orifice is approximately 0.3 l/min. The new set-up guarantees equal pressure in the bath and in the flow tube, but also that particles originating from the bath are sucked to the pump and are not registered by the optics. The modified CPC can stand pressure drops up to 50 hPa/s without its functioning is being affected for more than a few seconds.

Since the aircraft usually provides only 28 V DC power, the use of DC/DC-converters and modifications to the CPC electronics were necessary. Furthermore, a potentiometer was installed in the CPC electronics to select the temperature difference between the saturator and the condenser (originally fixed to 17°C) in the range of 5–19°C. As the temperature difference determines the supersaturation in the condenser, it is possible to shift the d_{50} towards larger or smaller diameters by reducing or increasing the temperature difference, respectively (cf. Section 3.2).

The CPCs modified in the above way are referred to as CPC 7610lp ("lp" stands for "low pressure") to distinguish them from the original instruments. To reach a d_{50} in the ultrafine particle size range, temperature differences larger than 19°C (maximum of the CPC 7610lp) are needed. Therefore, the CPC 7610ilp ("i" for "improved") was developed. In the CPC 7610ilp, a second Peltier element is installed and additional insulation was added, to increase the cooling capacity of the condenser. Due to these modifications, temperature differences of up to 27°C can be reached in the CPC 7610ilp.

2.2. Calibration set-up

The modified CPCs were calibrated with the low-pressure calibration set-up shown in Fig. 1. Polydisperse sodium chloride or silver aerosols with particle diameters of 5–70 nm and 3–50 nm, respectively, are produced in a tube furnace generator according to Scheibel and Porstendörfer (1983). After passing a dilution system, the operating pressure is reduced from ambient values to different flight level pressures (160–1000 hPa) using a needle valve as restrictor. The operating pressure is monitored by a piezoelectric pressure gauge. Downstream the valve, the aerosol enters a ^{241}Am bipolar charger. Afterwards, a quasi monodisperse fraction of the charged particles is selected out of the polydisperse aerosol in a DMA (Vienna type, short). For calibration, the DMA was operated with flow rates of 1 and 10 l/min (at laboratory pressure and temperature) for the aerosol and sheath air flow, respectively. To assure that the monodisperse aerosol leaving the DMA is distributed homogeneously over the transport tube, a mixing bottle is installed downstream the DMA. With the following three-way-valve system upstream the CPC, the spatial homogeneity of the aerosol is checked regularly, by swapping the CPC and AE flows.

The CPC counting efficiency is obtained by comparing the particle number concentration measured by the CPC with the reading of an aerosol electrometer (AE). Thereby, the time and pressure dependent AE-offset has to be considered, whereas the error due to multiple charged particles can be neglected compared to other experimental errors (Hermann, 2000). In the set-up, the AE flow rate is adjusted to the same value as the CPC flow rate to guarantee equal diffusive particle losses in the transport lines to the instruments. The airflow through the low-pressure part of the set-up is maintained by an oiled rotary vane vacuum pump.

The major difference between the low-pressure calibration set-up shown in Fig. 1 and set-ups described in the literature (e.g. Zhang & Liu, 1991) is that in former set-ups the particles are first charged and afterwards the operating pressure is reduced. Own experiments with this set-up type showed, however, that charged particles are accumulated at the needle of the pressure reducing valve (Hermann, 2000). Thereby, charges on passing particles are influenced. Although the exact mechanism is not known, as results wrong counting efficiency curves are obtained (e.g. a much lower counting efficiency for 50 nm particles compared to 20 nm particles). In the new set-up, the pressure is first reduced and afterwards the particles are bipolarly charged to prevent these

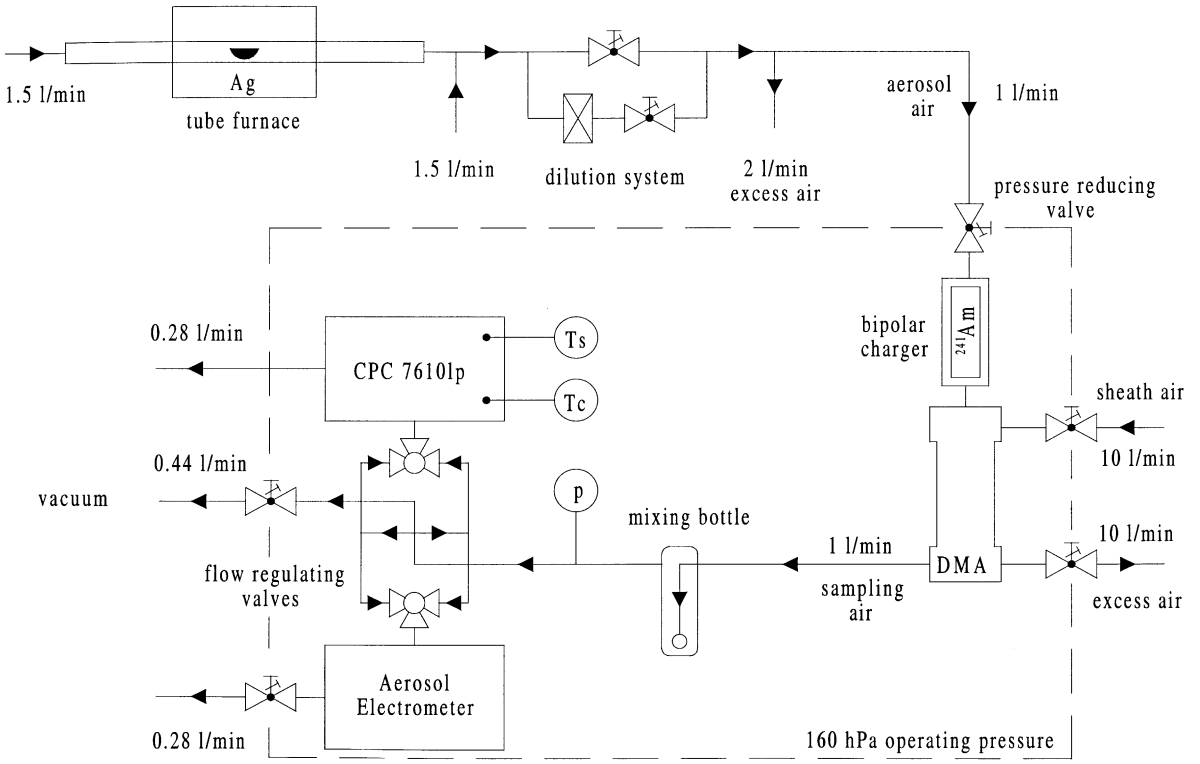

Fig. 1. Low-pressure calibration set-up. The sign "p" denotes a piezoelectric pressure gauge, "T_s" the saturator temperature sensor, and "T_c" the condenser temperature sensor. Downstream the pressure reducing valve, the set-up is operated at lower pressures down to 160 hPa. Volume flow rates are given at laboratory pressure and temperature.

charging effects. The new set-up implies, however, to operate a DMA at low pressure conditions which was reported for the first time in 1997 by Seto et al.

3. Results

3.1. Pressure dependence of the CPC counting efficiency

With the new calibration set-up, the CPC 7610lp counting efficiency was measured at six different pressures of 160, 200, 300, 400, 700 and 1000 hPa for particles of 5–50 nm diameter. The obtained counting efficiency curves are shown in Fig. 2. The x-axis error bars in the figure represent one standard deviation of the DMA transfer window (theoretical values, cf. Stolzenburg, 1988) and the y-axis error bars indicate the standard deviation of the counting efficiency mean values. These definitions are applied to all following figures.

Besides the experimental errors, the positions of the d_{50} shown in Fig. 2 are subject to a further uncertainty, which is caused by a small temperature variation in the CPC and is not included in the x-axis error bars. Since the CPC 7610 controls only the temperature difference and not the absolute

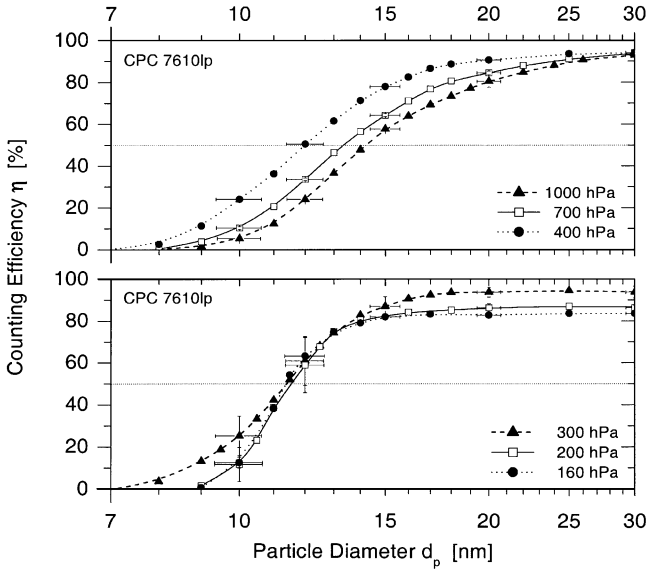

Fig. 2. CPC 7610lp counting efficiency at 160, 200, 300, 400, 700 and 1000 hPa. Error bars (not given for each point) indicate one standard deviation of the DMA transfer window (x-axis) and the standard deviation of the counting efficiency mean value (y-axis).

temperature of the saturator and condenser, the position of the d_{50} is also determined by the ambient temperature. For the CPC 7610 at laboratory temperatures between 18 and 30°C, a mean temperature difference range of 16.5–17.5°C was observed, which is within the uncertainty given by the manufacturer (17 $\pm$ 1°C). As it will be shown in the following section, this $\pm$ 0.5°C temperature variation around 17°C leads to an uncertainty in the d_{50} of approximately $\pm$ 0.5 nm.

Fig. 2 shows two important changes in the counting efficiency as the pressure decreases. First, a shift in the d_{50} towards smaller particle diameters, and secondly a decrease in the asymptotic maximum counting efficiency. The shift towards a smaller d_{50} is associated with an increasing slope as the pressure decreases. The direction of the shift implies that at lower pressure the heat transfer in the condenser increases more strongly than the butanol mass transfer to the walls. This results in higher supersaturations, and therefore, in lower detection limits.

Zhang and Liu (1990, 1991) have shown in their theoretical work on the CPCs 3020 and 3760 (the older version of the CPC 3760 is identical to the CPC 7610 used in this work) that there is a pressure dependence of the d_{50}. However, their data suggest a shift towards larger diameters as the pressure decreases. On the other hand, their calculations indicate that the shift in d_{50} should occur in the same direction, if either the pressure or the flow rate through the CPC is reduced. Wiedensohler et al. (1997) have shown, however, that the d_{50} of the CPC 7610/3760 shifts towards smaller particle diameters as the flow rate is reduced. Schröder and Ström (1997) conclude a similar behavior of the CPC 7610 at lower pressures as it is shown in Fig. 2 from their low flow calibration measurements. Furthermore, Wilson, Hyun, and Blackshear (1983) report a shift in the d_{50} towards smaller particle diameters for a pressure shift from 400 to 187 hPa, however, for a different CPC model. The pulse height analysis performed by Saros et al. (1996) with a CPC 3025 suggests a similar behavior. Their data imply an increase in the counting performance with decreasing

pressure from 1000 to 600 hPa and larger threshold diameters below 600 hPa. Measurements of the CPC 3760 counting efficiency with He as carrier gas performed by Niida, Wen, Udischas, and Kasper (1988) showed a shift of the d_{50} towards smaller particle diameters. Since the gas properties of air at reduced pressure are similar to those of He, the data of Niida et al. further confirm the results found in this study.

In summary, most former investigations evidence that the d_{50} of CPCs shifts towards smaller particle diameters as the pressure decreases, until at a certain pressure a minimum seems to be reached. This pressure threshold has different values for the various CPC models. For the CPC 7610lp/ilp used in this work, the minimum d_{50} is found in a broad pressure range of 160–300 hPa (cf. Fig. 2).

In Fig. 3, a comparison of the sparse experimental low-pressure data for the CPC 7610/3760 and the results of this study is shown. Although the data from Zhang and Liu (1991) agree well at 1000 hPa with the data of this work, at 200 hPa their counting efficiency curve is more flat and yields a much higher d_{50}. A reason for this discrepancy might be calibration set-up artifacts (cf. Section 2.2), whereas the difference in the aerosol material alone, i.e. silver in this study and sodium chloride used by Zhang and Liu, is not likely to account for this big difference (cf. Section 3.2).

Besides the data of Zhang and Liu (1991), the only other size-resolved low-pressure counting efficiency for the CPC 7610/3760 is reported by Cofer et al. (1998). This curve shows a lower counting efficiency and a larger d_{50} compared to the data of this work. A clear reason for this difference cannot be given.

The second important feature shown in Fig. 2 is the decrease of the asymptotic maximum counting efficiency with decreasing pressure. The reason for this behavior is not obvious. One possible explanation is that because the volume flow through the CPC decreases with decreasing pressure ($\sim 10\%$ at 200 hPa, experimental values, Hermann, 2000) the focusing nozzle at the

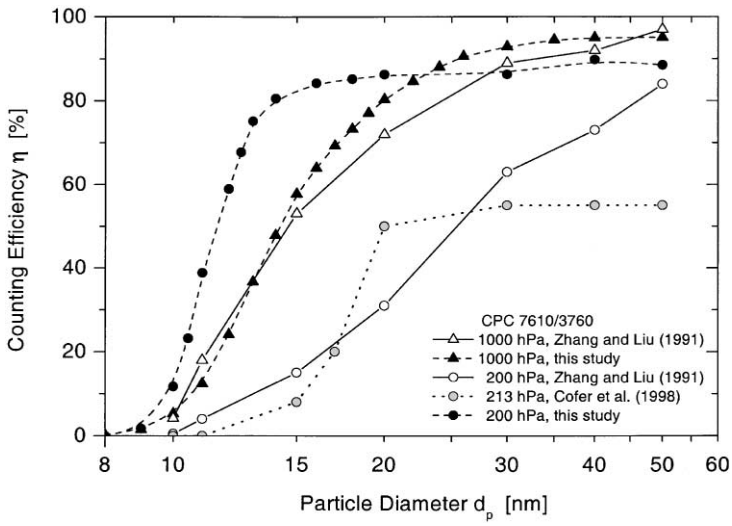

Fig. 3. CPC 7610/3760 low-pressure counting efficiencies at 200 hPa. Literature data are estimated from figures in the respective papers.

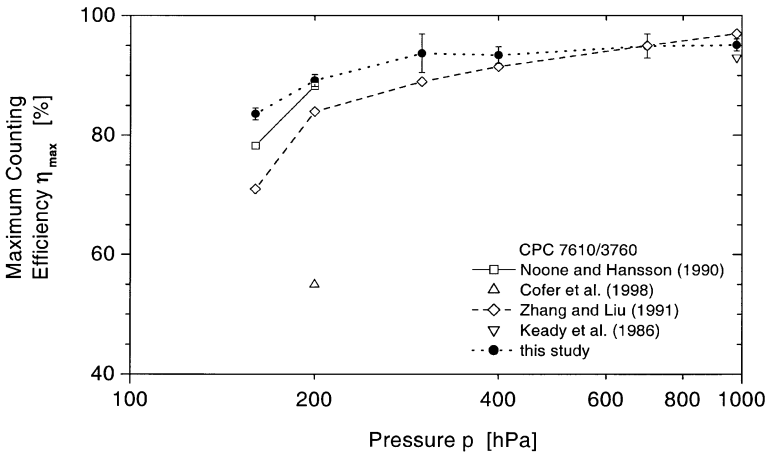

Fig. 4. CPC 7610/3760 maximum asymptotic counting efficiencies as function of operating pressure. All CPCs were operated at 17°C temperature difference. Literature data are estimated from figures in the respective papers.

optics entrance does not focus the aerosol flow properly anymore. Therefore, some particles may miss the viewing volume of the laser.

Fig. 4 compares the asymptotic maximum counting efficiencies measured in this work with values reported by Cofer et al. (1998), Keady, Quant, and Sem (1986), Noone and Hansson (1990), and Zhang and Liu (1991). The values of Keady et al., Noone and Hansson, and Zhang and Liu show only small deviations ($< 15\%$) from the values of this study, whereas the value of Cofer et al. is much lower.

3.2. Temperature dependence of the CPC counting efficiency

To derive information on the particle size distribution by a combination of similar CPCs, the threshold diameter d_{50} of the individual devices has to be changed. Of all adjustable operating parameters the temperature difference between the saturator and condenser has the strongest influence on d_{50} (Zhang & Liu, 1990). In a previous study, McDermott, Ockovic, and Stolzenburg (1991) investigated this dependency for a modified CPC 3025. For the TSI Model 3010, Mertes, Schröder, and Wiedensohler (1995), Russell et al. (1996), and Wiedensohler et al. (1997) report shifts in the d_{50} for temperature differences between 17 and 36°C. The CPC 7610/3760 used in this study was investigated by Schröder and Ström (1997) at 18 and 28°C temperature difference, but only at normal pressure. Up to now, there are no data published on the temperature dependence of the CPC 7610/3760 counting efficiency at lower pressures.

CPC 7610lp and CPC 7610ilp counting efficiencies were investigated at temperature differences of 10.5, 12, 17, 20, and 26°C at 200 hPa operating pressure (Fig. 5). Curves for 20°C and 26°C depict measurements with the CPC 7610ilp and Ag particles. The 10.5, 12, and 17°C curves are obtained using the CPC 7610lp. For 12 and 17°C, Ag particles were used while the 10.5°C curve was measured for NaCl particles. The use of sodium chloride became necessary, since silver particles larger than approximately 50 nm could not be generated in a sufficient high number concentration (> 1000 particle/cm^3) to obtain an acceptable signal to noise ratio in the AE.

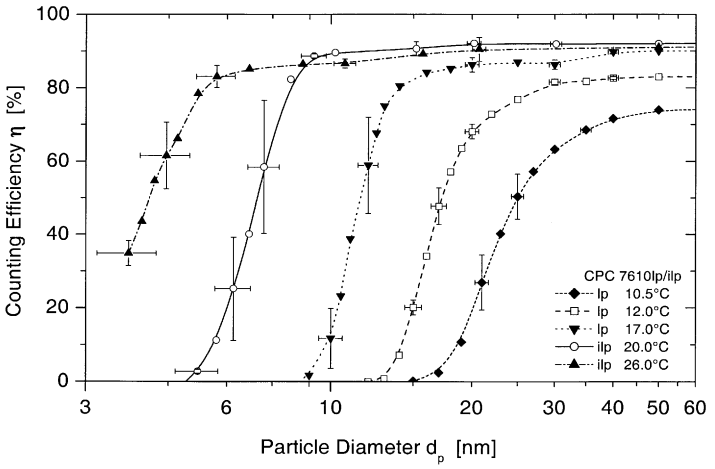

Fig. 5. Counting efficiency curves of the CPC 7610lp and CPC 7610ilp for 10.5, 12, 17, 20, and 26°C temperature difference. Operating pressure is 200 hPa. Measurements were performed with either NaCl particles (10.5°C) or Ag particles (other curves).

In Fig. 5, the counting efficiency curves for 20 and 26°C have been corrected for diffusion effects. For ultrafine particles, the size window of the DMA, i.e. the size range of particles able to pass the DMA, is enlarged due to diffusion broadening. Particularly, at lower pressures this effect is enhanced and the DMA window is relatively broad ($\pm$ 10% in particle diameter at 5 nm). Since the slopes of the particle size distribution generated by the tube furnace and of the CPC counting efficiency curve are very steep in the range from 3 to 8 nm, the majority of particles measured by the CPC are particles at the lower mobility (larger particle diameter) limit of the DMA window. For these particles, however, the counting efficiency is higher. Thereby, the measured counting efficiency (i.e. the average over the DMA window) becomes higher than the real counting efficiency for the selected particle diameter. To account for this diffusion effect and correct the data, the diffusion broadening was calculated according to the DMA-theory given by Stolzenburg (1988). His theory was confirmed for the DMA type used in this work by experimental results of Reischl, Mäkelä, and Necid (1998). For the 20 and 26°C curves, a shift of approximately 0.2 and 0.7 nm, respectively, towards larger particle diameters results and was applied to the data.

Fig. 5 shows two important features of the counting efficiency: first a shift of the d_{50} towards smaller particle diameters with increasing temperature difference and secondly a decrease in the asymptotic maximum counting efficiency with decreasing temperature difference.

The shift of the d_{50} towards smaller particle diameters with increasing temperature difference and the simultaneous increase in the slope is explained by higher supersaturations achieved in the condenser. It should be noted, however, that the shift between the 17 and 20°C curves is partly induced by the differences in the used CPC types, i.e. "lp" and "ilp". Furthermore, the use of NaCl particles for the 10.5°C curve instead of Ag particles, accounts for a slight shift of approximately 1 nm towards larger particle diameters for the d_{50} of this curve (see below). It is obvious that there is an influence of particle material and shape on the particle activation in the CPC, and therefore,

on the position of the d_{50}. The question is, however, how large is this influence for different particle materials and what are the implications for measurements.

Sinclair (1982) gives an overview of investigations performed with several older types of CPCs and their counting efficiencies as a function of particle material. For the CPC 3025, Kesten, Reineking, and Porstendörfer (1991) report a difference of less than 1 nm in the curves for Ag and NaCl particles, where Ag shows the lower d_{50}. A similar picture is given by Schröder and Ström (1997) for the CPC 7610. In their study, the shift in the d_{50} is slightly larger than 1 nm. Own experiments for the CPC 7610lp at 17°C temperature difference and 200 hPa operating pressure (not shown here) yielded that the NaCl-curve is shifted approximately 1.4 nm towards larger particle diameters compared to the Ag-curve. This difference might be attributed to different particle shapes or wettabilities of both materials with butanol.

As the majority of the submicrometer upper tropospheric particles consists of H_2SO_4/H_2O (Yamato & Ono, 1989; Sheridan, Brock, & Wilson, 1994), it is interesting to compare counting efficiencies obtained with NaCl or Ag to those obtained with H_2SO_4. For a CPC 3020, Madelaine and Metayer (1980) showed that there are differences in the counting efficiency curves for NaCl, H_2SO_4, and V_2O_5 particles. According to their results, H_2SO_4 particles yield the highest counting efficiency and a d_{50} which is approximately 3 nm smaller than the d_{50} obtained with NaCl particles. Saros et al. (1996) interpreted the small difference they found in the activation of H_2SO_4 and NaCl particles in a CPC 3025 to be caused by the different shape of the particles. According to these two studies, the in-flight 50% particle detection diameters of the CPCs should be equal or even 1–2 nm smaller than the ones measured in this study.

Looking at the d_{50} position of the different curves in Fig. 5, it is conspicuous that towards larger temperature differences the shift in the d_{50} per degree Celsius is reduced. This behavior can be explained by theoretical considerations based on the Kelvin effect concerning the particle activation in the condenser. A short calculation shows that the temperature difference ΔT necessary to activate a certain particle diameter d_p is nearly proportional to $1/d_p$. To support this theory, the d_{50} was measured as a function of temperature difference for the CPC 7610ilp and CPC 7610lp at 200 hPa operating pressure. Fig. 6 shows the obtained results together with the relation $d_{50} \sim 1/\Delta T$. For the CPC 7610ilp, the measured particle diameters follow the $1/\Delta T$-relation quit well, whereas the CPC 7610lp data show little deviations from this approximation. By means of the results displayed in Fig. 6, it is possible to predict the position of the d_{50} if the temperature difference in the CPC is known.

To investigate how much the position of the d_{50} changes for different flight levels (i.e. pressures), additional experiments have been carried out at 300 hPa and 12, 17, and 26°C. In Fig. 7, the results for 300 hPa are compared with the data at 200 hPa. For 26 and 17°C, the respective curves show only small deviations in the d_{50}, whereas a difference of about 1 nm was observed for 12°C. Considering the CPC 7610lp calibration results at 17°C and various pressures (cf. Fig. 2), it can be stated that the variation of the d_{50} is small for the pressure range encountered during level flight (160–300 hPa) for both CPC types.

The second important feature of the counting efficiencies shown in Fig. 5, is the decrease in the asymptotic maximum counting efficiency with decreasing temperature difference. As the temperature differences decreases, the volume in the condenser where the supersaturation is sufficiently high for particle activation becomes smaller. Consequently, an increasing number of particles do not grow and are not counted by the optics. As this effect becomes only significant for temperature

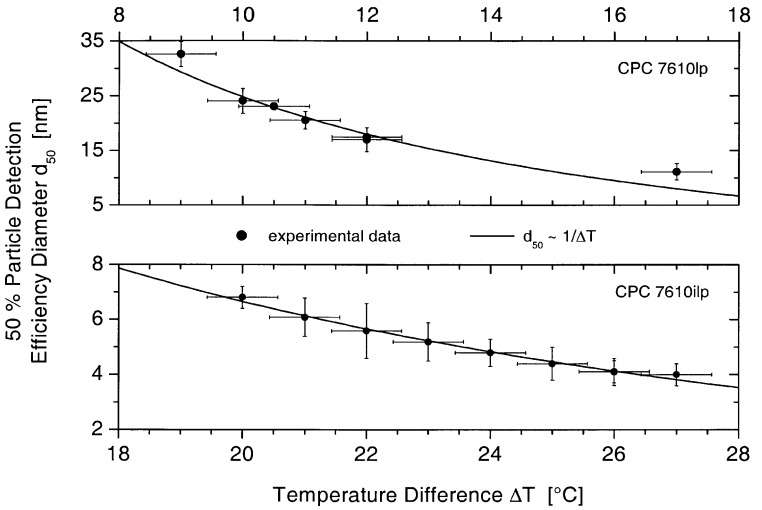

Fig. 6. Fifty percent particle detection efficiency diameter d_{50} of the CPC 7610ilp and CPC 7610lp as function of temperature difference ΔT. The solid line denotes the relation $d_{50} \sim 1/\Delta T$. Measurements were performed at 200 hPa operating pressure. Error bars indicate the experimental uncertainty of the temperature measurement (x-axis) and the standard deviation of the mean d_{50} values (y-axis).

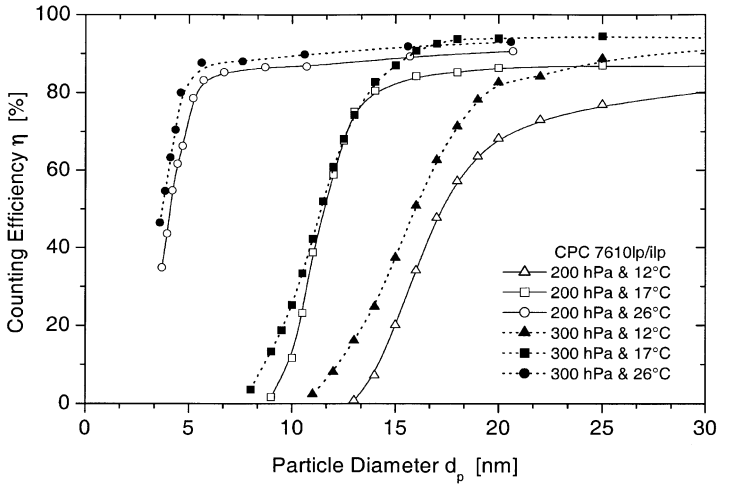

Fig. 7. CPC 7610lp/ilp counting efficiency at 200 and 300 hPa operating pressure and 12, 17, and 26°C temperature difference.

differences below 17°C (cf. Fig. 5), further investigations were performed only for the CPC 7610lp. The obtained results are shown in Fig. 8. In this context, the asymptotic maximum counting efficiency was defined as the counting efficiency at 70 nm.

Fig. 8 shows a continuous decrease in the asymptotic maximum counting efficiency with decreasing temperature difference. Below a temperature difference of 10°C, the CPC 7610lp can no

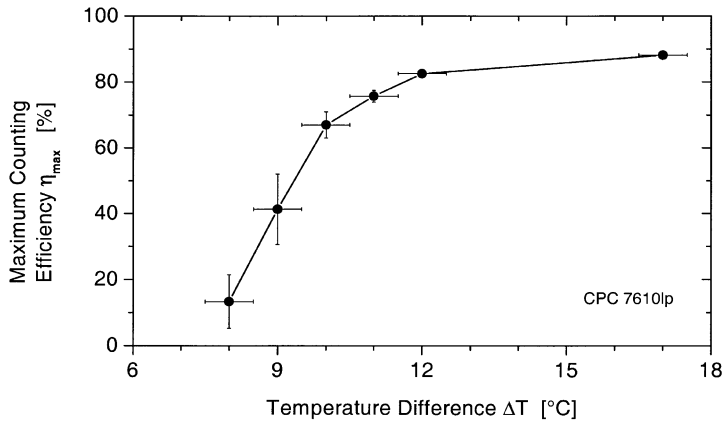

Fig. 8. CPC 7610lp maximum counting efficiency as function of temperature difference ΔT. Measurements were performed with 70 nm particles at 200 hPa operating pressure.

longer be operated soundly, since a small change of $\pm$ 0.5°C in the temperature difference results in a maximum counting efficiency change of more than 70%. On account of this lower temperature limit, the maximum d_{50} which can be achieved with the CPC 7610lp is approximately 23 nm (cf. Fig. 6).

3.3. Particle coincidence

The CPC 7610 optics works in the so called "pulse count mode" where every particle event produces an output pulse. At higher particle number concentrations, the probability of two particles coinciding in the viewing volume of the laser increases rapidly. The pulses caused by these particles overlap and the coinciding particles are counted as one. This coincidence effect is well known and can be considered during data evaluation. The true particle number concentration N_{true} can be calculated from the measured particle concentration $N_{\text{meas.}}$ according to (TSI 7610 Instruction Manual)

$$N_{\text{true}} = N_{\text{meas.}} \exp(N_{\text{true}} Qt) = N_{\text{meas.}} \exp(N_{\text{true}} c), \tag{1}$$

where Q is the volume flow rate through the CPC ($\approx$ 24 cm^3/s), t the time each particle stays in the viewing volume ($\approx$ 0.25 μs), and c a coincidence parameter, which is given by the product Qt.

The manufacturer of the CPC 7610 gives an upper concentration range limit due to coincidence of approximately 10^4 particles/cm^3 (6% coincidence error, cf. TSI 7610 Instruction Manual). However, Yamada and Koizumi (1992) showed that it is possible to extend this range by calibration to over 10^5 particles/cm^3. For the CPC 7610lp and CPC 7610ilp, calibration experiments were performed to assess the coincidence effect at higher particle number concentrations. These investigations were carried out with the set-up shown in Fig. 1 at 200 hPa operating pressure. Thereby, AE current and CPC counts are measured for different concentrations at fixed particle diameters (16 and 20 nm for the CPC 7610lp, 12 nm for the CPC 7610ilp). The particle number concentration obtained by the AE is considered to give the true particle concentration N_{true},

whereas the CPC reading yields the $N_{\text{meas.}}$ value. Thereby, the maximum counting efficiencies of the CPCs had to be considered. The results of the calibration experiments are shown in Figs. 9 and 10.

Since Eq. (1) is an implicit function and cannot be solved directly to N_{true}, the equation was Taylor-expanded up to the second order to obtain a function by which N_{true} can be calculated easily. The resulting function is shown in Eq. (2). The error due to this Taylor-expansion is less than 2% for particle concentrations up to 50,000 particles/cm^3.

$$N_{\text{true}} = \frac{1}{c^2}\left(\frac{1}{N_{\text{meas.}}} - c\right) - \sqrt{\left(\frac{1}{c^2}\left(\frac{1}{N_{\text{meas.}}} - c\right)\right)^2 - \frac{2}{c^2}}. \tag{2}$$

To obtain the coincidence parameter c, which is normally given by the product of the volume flow rate Q and the residence time t (cf. Eq. (1)), for both CPCs a curve of the form given in Eq. (2) was fitted to the experimental data.

The fitting procedures yielded coincidence parameters of $c_{\text{lp}} = 7.8\text{E-}6$ cm^3 ($\pm$ 10%) and $c_{\text{ilp}} = 10.6\text{E-}6$ cm^3 ($\pm$ 15%) for the CPC 7610lp and CPC 7610ilp, respectively. These values are higher than the value for the original CPC 7610 with $c = 5.9\text{E-}6$ cm^3 (TSI 7610 Instruction Manual), although neither the volume flow rate nor the residence time were changed in that order of magnitude for both CPCs. The larger coincidence parameter of the CPC 7610ilp is attributed to the larger supersaturations in the condenser, which leads to larger particles and hence to higher and wider particle pulses. Consequently, coincidence is increased. For the CPC 7610lp, the larger coincidence parameter is caused by the data acquisition system, which smears and broadens the output pulses. Therefore, the two coincidence curves shown in Figs. 9 and 10 are representative only for the specific CPCs of this study. By using Eq. (2) and the obtained coincidence parameters,

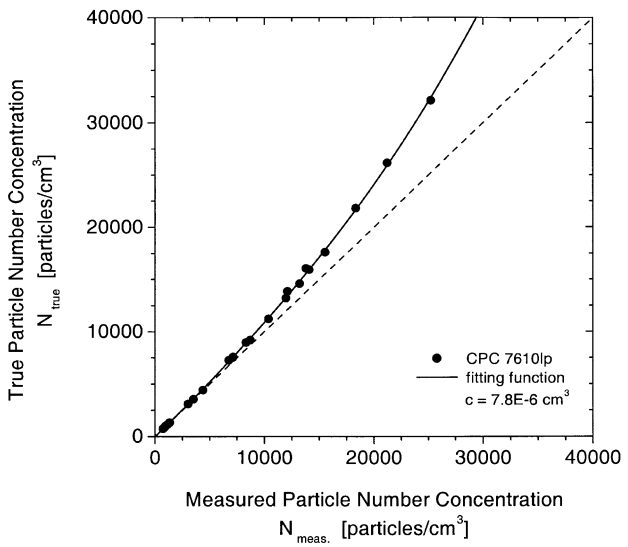

Fig. 9. Particle coincidence curve for the CPC 7610lp. The solid line shows a fitting function to the measurement points according to Eq. (2). The dotted curve indicates the one to one line. "c" gives the coincidence parameter defined in Eq. (1).

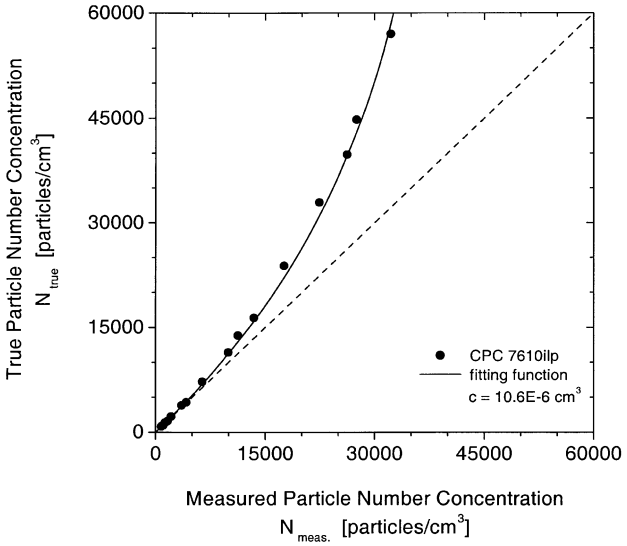

Fig. 10. Particle coincidence curve for the CPC 7610ilp. Same representation as Fig. 9.

the concentration ranges for the CPC 7610lp and CPC 7610ilp can be extended to 40,000 and 60,000 particles/cm^3, respectively.

4. Example of particle measurements

"As an illustrative example for an application of a low-pressure CPC combination as fast particle counting system, aircraft measurements taken abroad a commercial aircraft within the scope of the CARIBIC project are shown (cf. Brenninkmeijer et al, 1999). In CARIBIC, three CPCs 76101p/ilp are operated in parallel at 12°C, 17°C, and 27°C temperature difference. Accordingly, these counters yield particle number concentrations for particles larger than approximately 4, 12, and 18 nm diameter, respectively. These threshold diameters can vary by $\pm$ 1 nm during level flight, dependent on ambient temperature, operating pressure, and chemical composition of the measured particles. The upper threshold particle diameter of approximately 1.25 mm (d50, Stokes diameter, rparticle = 1.55 g/cm^3, Hermann et al. 2001) is determined by the aerosol inlet system and was experimentally derived. Assuming rectangular functions for the CPC counting efficiencies, the readings of the first two counters can be subtracted to yield the ultrafine particle number concentration (4–12 nm). This induces, however, an uncertainty in the ultrafine particle number of concentration which depends on the actual particle size distribution. By operating the third CPC in combination with a pre-impactor, which sets and upper threshold diameter of approximately 135 nm at flight level pressure, this counter is restricted to Aitken mode particles (18–135 nm)."

Fig. 11 shows particle number concentrations measured during a four minute time interval on a flight from Düsseldorf/Germany to Male/Maldives on March 25, 2000. At the given time, the

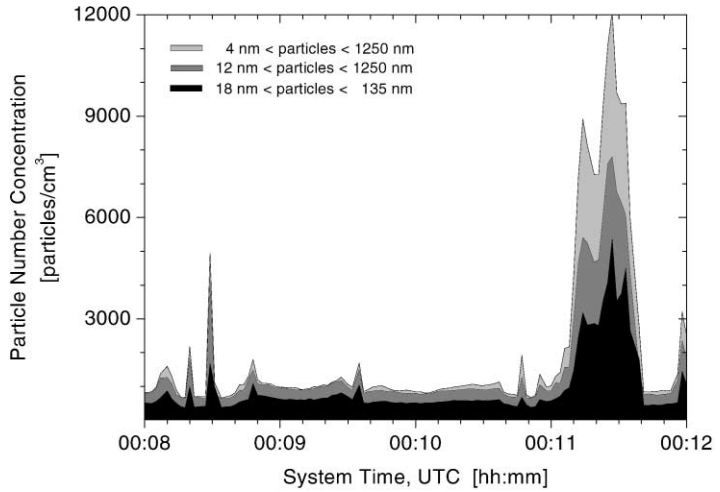

Fig. 11. Particle number concentrations measured with 2 s time resolution on a flight from Düsseldorf/Germany to Male/Maldives on March, 25th, 2000. Flight altitude was 37 000 feet, which corresponds to a pressure of 216 hPa. Concentration values are corrected for particle coincidence, CPC counting efficiency, and inlet transmission efficiency and are transformed to standard conditions (1013.25 hPa, 273.15 K).

aircraft flew at 37,000 feet altitude over the Iran (30.9°N, 52.4°E). The 4-min period covers a horizontal range of approximately 60 km. The time resolution of the measurement is 2 s, corresponding to a horizontal resolution of ca. 500 m. Particle number concentrations in the figure are corrected for particle coincidence, pressure dependent CPC counting efficiencies, and inlet system sampling efficiency (cf. Hermann et al., 2000). For easier comparison, the concentrations are transformed to standard conditions (STP: 1013.25 hPa, 273.15 K).

Fig. 11 shows that sometimes small structures of only 4 s duration can be found in upper tropospheric particle number concentrations. Even larger particle peaks, like the one occurring shortly after 00:11 UTC, can last only 40 s and are finely structured. These data emphasize the need for fast particle measurement systems as well as for fast trace gas and meteorological measurement systems in order to interpret the observed particle data properly.

5. Summary

In the present paper, we described the modification and calibration of three CPCs 7610 for low-pressure conditions. The commercially available CPCs were modified with respect to environmental conditions and aviation requirements. Furthermore, the 50% particle detection diameters of the CPCs were changed to obtain a certain sizing capability with the CPC combination. These modifications were achieved by either increasing or decreasing the temperature difference between the saturator and condenser block inside the CPC.

The modified CPCs 7610 were tested for their operational properties, particularly their low-pressure counting efficiency. Therefore, a new calibration set-up was built, including a DMA

operated at low pressures. With this calibration set-up, the CPC counting efficiency was investigated as a function of operating pressure (160–1000 hPa) and temperature difference between saturator and condenser (10.5–26°C). The obtained results show that the modified CPCs work properly at pressures down to 160 hPa. Furthermore, the counting efficiency curve of the instruments shifts to smaller particle diameters and becomes steeper by reducing the operating pressure or increasing the temperature difference in the CPCs. The threshold diameter of the modified instruments can be adjusted between 4 nm and 23 nm at operating pressures between 160 hPa and 300 hPa. In further experiments, particle coincidence in the CPC optics was studied. With the obtained results, the upper concentration range limit of 10,000 particles/cm^3 for the CPCs (manufacturers specification) could be extended to more than 40,000 particles/cm^3.

Acknowledgements

The authors are grateful for the technical and financial support of the CARIBIC project by LTU International Airways and the Environmental Technologies RTD Program of the Commission of the European Communities DG XII under contract number ENV4-CT95-0006. Furthermore, we acknowledge the technical support by H. Haudek and the helpful discussions with F. Stratmann and J. Heintzenberg.

References

Brenninkmeijer, C. A. M., Crutzen, P. J., Fischer, H., Güsten, H., Hans, W., Heinrich, G., et al. (1999). CARIBIC Civil aircraft for global measurement of trace gases and aerosols for the tropopause region. *J. Atmos. Oceanic Technol.*, *16*, 1373–1383.

Brock, C. A., Schröder, F., Kärcher, B., Petzold, A., Busen, R., & Fiebig, M. (2000). Ultrafine particle size distribution in aircraft exhaust plumes. *Journal of Geophysical Research*, *105*, 26,555–26,567.

Clarke, A. D. (1993). Atmospheric nuclei in the pacific midtroposphere: Their nature, concentration, and evolution. *Journal of Geophysical Research*, *98*, 20,633–20,647.

Cofer, W. R., Anderson, B. E., Winstead, E. L., & Bagwell, D. R. (1998). Calibration and demonstration of a condensation nuclei counting system for airborne measurements of aircraft exhausted particles. *Atmospheric Environment*, *32*, 169–177.

Dreiling, V., & Jaenicke, R. (1988). Aircraft measurement with condensation nuclei counter. *Journal of Aerosol Science*, *19*, 1045–1050.

Heintzenberg, J., & Ogren, J. A. (1985). On the operation of the TSI-3020 condensation nuclei counter at altitudes up to 10 km. *Atmospheric Environment*, *19*, 1385–1387.

Hermann, M. (2000). *Development and application of an aerosol measurement system for use on commercial aircraft*. Ph.D. thesis, Universität Leipzig, 2000.

Hermann, M., Stratmann, F., Wilck, M., & Wiedensohler, A. (2001). Sampling characteristics of an aircraft-borne aerosol inlet system. *Journal of Atmospheric and Oceanic Technology*, *18*, 7–19.

Keady, B. P., Quant, F. R., & Sem, J. S. (1986). A small, high-flow condensation nucleus counter for clean room particle monitoring. Poster presented at the *2nd international conference AAAR-GAeF*, West-Berlin, Germany, September 22–26.

Kesten, J., Reineking, A., & Porstendörfer, J. (1991). Calibration of a TSI model 3025 ultrafine condensation particle counter. *Aerosol Science and Technology*, *15*, 107–111.

Madelaine, G., & Metayer, Y. (1980). Note. *Journal of Aerosol Science*, *11*, 358.

McDermott, W. T., Ockovic, R. C., & Stolzenburg, M. R. (1991). Counting efficiency of an improved 30 Å condensation nucleus counter. *Aerosol Science and Technology*, *14*, 278–287.

Mertes, S., Schröder, F., & Wiedensohler, A. (1995). The particle detection efficiency curve of the TSI 3010 CPC as a function of the temperature difference between saturator and condenser. *Aerosol Science and Technology*, *23*, 257–261.

Niida, T., Wen, H. Y., Udischas, R., & Kasper, G. (1988). Counting efficiency of condensation nuclei counters in N_2, Ar, CO_2 and He. *Journal of Aerosol Science*, *19*, 1417–1420.

Noone, K. J., & Hansson, H. -C. (1990). Calibration of the TSI 3760 condensation nucleus counter for nonstandard operating conditions. *Aerosol Science and Technology*, *13*, 478–485.

Reischl, G. P., Mäkelä, J. M., & Necid, J. (1998). Performance of the Vienna type differential mobility analyzer at 1.2–20 nanometer. *Aerosol Science and Technology*, *27*, 651–672.

Russell, L. M., Zhang, S. -H., Flagan, R. C., Seinfeld, J. H., Stolzenburg, M. R., & Caldow, R. (1996). Radially classified aerosol detector for aircraft-based submicron aerosol measurements. *Journal of Atmospheric and Oceanic Technology*, *13*, 598–609.

Saros, M. T., Weber, R. J., Marti, J. J., & McMurry, P. H. (1996). Ultrafine aerosol measurement using a condensation nucleus counter with pulse height analysis. *Aerosol Science and Technology*, *25*, 200–213.

Scheibel, H. G., & Porstendörfer, J. (1983). Generation of monodisperse Ag- and NaCl aerosols with particle diameters between 2 and 300 nm. *Journal of Aerosol Science*, *14*, 113–126.

Schröder, F., & Ström, J. (1997). Aircraft measurements of sub micrometer aerosol particles (> 7 nm) in the midlatitude free troposphere and tropopause region. *Atmospheric Research*, *44*, 333–356.

Seto, T., Nakamoto, T., Okuyama, K., Adachi, M., Kuga, Y., & Takeuchi, K. (1997). Size distribution measurement of nanometer-sized aerosol particles using DMA under low pressure conditions. *Journal of Aerosol Science*, *28*, 193–206.

Sheridan, P. J., Brock, C. A., & Wilson, J. C. (1994). Aerosol particles in the upper troposphere and lower stratosphere: Elemental composition and morphology of individual particles in northern midlatitudes. *Geophysical Research Letters*, *23*, 2587–2590.

Sinclair, D. (1982). Particle size sensitivity of condensation nucleus counters. *Atmospheric Environment*, *16*, 955–958.

Stolzenburg, M. R. (1988). *An ultrafine aerosol size distribution measuring system*. Ph.D. thesis, Mechanical Engineering Department, University of Minnesota, Minneapolis, USA, 1988.

Wiedensohler, A., Orsini, D., Covert, D. S., Coffmann, D., Cantrell, W., Havlicek, M., Brechtel, F. J., Russell, L. M., Weber, R. J., Gras, J., Hudson, J. G., & Litchy, M. (1997). Intercomparison study of size-dependent counting efficiency of 26 condensation particle counters. *Aerosol Science and Technology*, *27*, 224–242.

Wilson, J. C., Hyun, J. H., & Blackshear, E. D. (1983). The function and response of an improved stratospheric condensation nucleus counter. *Journal of Geophysical Research*, *88*, 6781–6785.

Yamada, Y., & Koizumi, A. (1992). Particle coincidence error in pulse count mode of CNC. *Journal of Aerosol Science and Technology, Japan*, *7*, 240–244.

Yamato, M., & Ono, A. (1989). Chemical and physical properties of stratospheric aerosol particles in the vicinity of tropopause folding. *Journal of the Meteorological Society of Japan*, *67*, 147–165.

Zhang, Z. Q., & Liu, B. Y. H. (1990). Dependence of the performance of TSI 3020 condensation nucleus counter on pressure, flow rate, and temperature. *Aerosol Science and Technology*, *13*, 493–504.

Zhang, Z., & Liu, B. Y. H. (1991). Performance of TSI 3760 CNC at reduced pressures and flow rates. *Aerosol Science and Technology*, *15*, 228–238.